Mixing Efficiency of Rough Channels

Francis Ninh

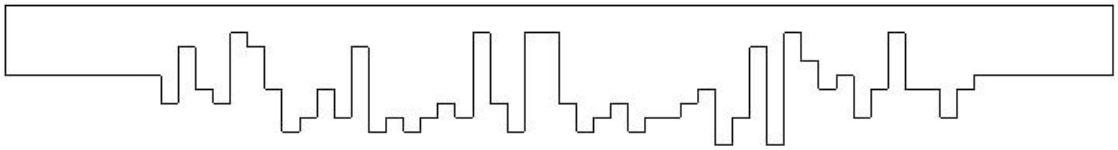

Abstract

The purpose of the following project was to achieve the most efficient mixing in a micro fluidic device by developing different variations of two parallel plates with one containing random ridges. Variances in concentrations were used to describe how effective the mixing was. The solutions were obtained through COMSOL Multiphysics by solving the local Navier-Stokes and convection-diffusion equations. It was found that these ridges did not improve mixing when compared to flow between to flat plates. However, when the ridges were allowed to extend into channel creating choke points the mixing improved and were found to be much more efficient at lower Peclet numbers when compared to flow between two flat plates. Two and three dimensional flows were examined in this geometry and it was found that the two dimensional was representative. This study involved Peclet numbers from 100 to 1000 and Reynolds number of one.

Introduction

Dispersion of a tracer in 2D flow between two parallel plates has been found to increase when random ridges are added to one of the plates[1], as shown in Figure 1.

Figure 1: Section of the channel containing random ridges on one plate[1]. Figure is scaled by a factor of four in the vertical direction.

The purpose of the following was to obtain a variation of the channel shown in Figure 1 that would achieve the most efficient mixing.

To describe the mixing, the variance of concentration is used[2]:

$$C_{varaince} = \frac{\int_A \left[c(x,y) - c_{mixingcup}\right]^2 v(x,y)dxdy}{\int_A v(x,y)dxdy} \quad \textbf{(1)}$$

where $c_{mixingcup}$ is defined as the concentration of fluid if the flow emptied into a cup that was well stirred[2]:

$$C_{mixing\ cup} = \frac{\int_A c(x,y)v(x,y)dxdy}{\int_A v(x,y)dxdy} \quad \textbf{(2)}$$

Optical measurements that are made through a thin layer of a microfluidic device[2] will also be considered:

$$C_{optical} = \frac{\int_0^L c(x,y,z)dy}{\int_0^L dy} \quad \textbf{(3)}$$

$$C_{optical} = \frac{\int_A \left[c(x,y) - c_{optical}\right]^2 dxdy}{\int_A dxdy} \quad \textbf{(4)}$$

Since optical measurements do not take into account a non-uniform velocity profile, mean concentrations obtained from optical measurements may differ from those of the mixing cup concentration. Thus these mean concentrations and their respective variances will be compared to see if optical measurements would be appropriate in this geometry. Along with the mean concentrations and variances, pressure drops will also be evaluated at a Reynolds, number of 1

and over a range of Peclet numbes. The range of Pe we will be dealing with is from 100-1000. Reynolds and Peclet numbers are defined respectively:

$$\mathrm{Re} \equiv \frac{\rho \langle v \rangle l_c}{\eta}$$

$$Pe \equiv \frac{v l_c}{D}$$

and where the characteristic length l_c is defined as the width of the inlet.

The most efficient mixer developed from Figure 1 will then be examined in three dimensions.

Method

COMSOL was used to solve the Navier-Stokes and convection-diffusion equations in their non-dimensional forms respectively[3]:

$$\mathrm{Re}\frac{\partial \mathbf{u}}{\partial t} + \mathrm{Re}\,\mathbf{u} \cdot \nabla \mathbf{u} = -\nabla p + \nabla^2 \mathbf{u}$$

$$\frac{\partial c}{\partial t} + \mathbf{v} \cdot \nabla c = \frac{1}{Pe} \nabla^2 c$$

COMSOL was then used to compute the mixing cup and optical concentrations, their respective variances, and pressure drops across the channel.

The boundary conditions set on all models are as follow:

Navier-Stokes

1) The inlet was assumed to be fully developed flow with an average velocity of 1 m/s.
2) Outlet pressure was set to zero
3) No slip condition was assumed

Convection-Diffusion

4) The inlet concentration was set to zero on the upper half of the inlet and on the bottom half the concentration was set to 1.
5) The outlet boundary chosen was convective flux.

Geometries

The following structures developed have the following dimensions in common:

Width of Inlet	1
Total Channel Length	20
Rough Channel Length	12

Table 1: Listed dimensions common to all geometries.

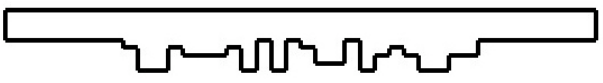

(A)

(B) (C)

Figure 2: All geometries were assigned random ridges. The widths (W) of the ridges were kept constant throughout each model but the height (H) was determined randomly. All ridges extend down to a maximum of the width of the channel (1 unit). In (c) however, the ridges are allowed to extend above the bottom of the plate to a maximum of .6 units. (A) W of ridge = .5, H of ridge = n(.25) (B) W = .25 H = n(.25) (C) W = .25, H =(n).2. Where n is a random integer and of values from 0 to a value where H was no greater than width of the inlet.

The widths of the ridges were predetermined while the heights of the ridges were randomly assigned over the entire channel. To assign the height dimensions to the ridges a pseudo-random numbers were generated from the MATLAB function "ceil". These integers were then multiplied by a fraction, which was predetermined, of the inlet width. The maximum height allowed for each ridge was the width of the inlet. Figure 2 depicts the three geometries produced from this method.

Figure C was found to be the most efficient mixer and was examined in three dimensions by extruding it in the third dimension by 1 unit as shown in Figure 3. This third dimension will be referred to as y. For this 3D geometry the inlet and outlets were shortened by two units each.

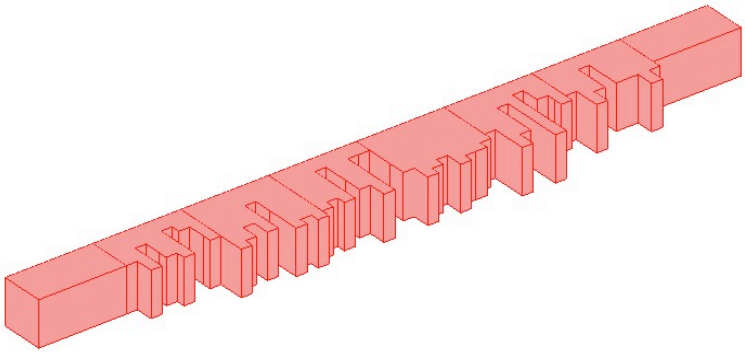

Figure 3: The channel was extruded in COMSOL by one unit in the y dimeonson. The inner boundaries depicted in the figure above were placed to evaluate concentrations and variances at the particular section and did not affect the flow.

Results

In geometries A and B the variances calculated for the range of Peclet numbers were greater than the variances in the case of no ridges in either plate. However, the variances were lower in geometry C where the ridges were allowed to extend into the channel. Table 2 lists the variances at Pe of 100 and 1000.

Pe #	Flat Plates	Geometry A	Geometry B	Geometry C
100	8.45E-04	1.53E-03	1.18E-03	1.27E-04
1000	0.114	0.121	0.118	0.0941

Table 2: Variances for each geometry at Peclet number 100 and 1000.

Although geometry C has achieved the best mixing the pressure drop across the inlet and outlet is the greatest among the four considered. Table 3 displays the pressure drops for all four geometries.

Pressure Drop (Pa)			
Flat Plates	Geometry A	Geometry B	Geometry C
6.00	4.54	5.17	23.2

Table 3: Pressure drop (Pa) of all geometries.

The variances calculated from the optical measurements over the entire range of Peclet numbers and for all geometries are greater than the variances calculated from c_{mix}. However, the relative values from geometry to geometry are consistent. That is, geometry C still has the lowest variances. Table 4 lists the variances calculated from the optical concentration.

Pe #	Flat Plates	Geometry A	Geometry B	Geometry C
100	1.13E-03	2.05E-03	1.58E-03	1.34E-03
1000	0.145	0.152	0.15	0.123

Table 4: Optical variances of all geometries at Peclet number 100 and 1000.

In order to obtain a solution in 3D that did not contain solutions with unrealistic oscillations the inlet and outlets were shortened by two units. Table 5 summarizes the findings of geometry C with the shortened inlets and outlets.

	Mixing Cup Variances		Optical Variances	
Pe #	Geometry C	Geometry C (3D)	Geometry C	Geometry C (3D)
100	3.74E-04	2.99E-04	5.01E-04	3.69E-04
1000	0.104	0.0946	0.136	0.114

The pressure drops are 22.0 and 31.8 Pa for the 2D and 3D geometries respectively.

Discussion

The most efficient mixing obtained was that of the geometry which the ridges protruded into the channel. All graphs and discussion in the following will only involve this particular geometry.

To compare the variances of different geometries, one must consider not only the Peclet number but also the length along which the fluid is allowed to mix. If we consider the ratio of the path length to the Peclet number the variances are equivalent for that particular geometry regardless of the Peclet number, see Figure 4 for variances across the rough channel.

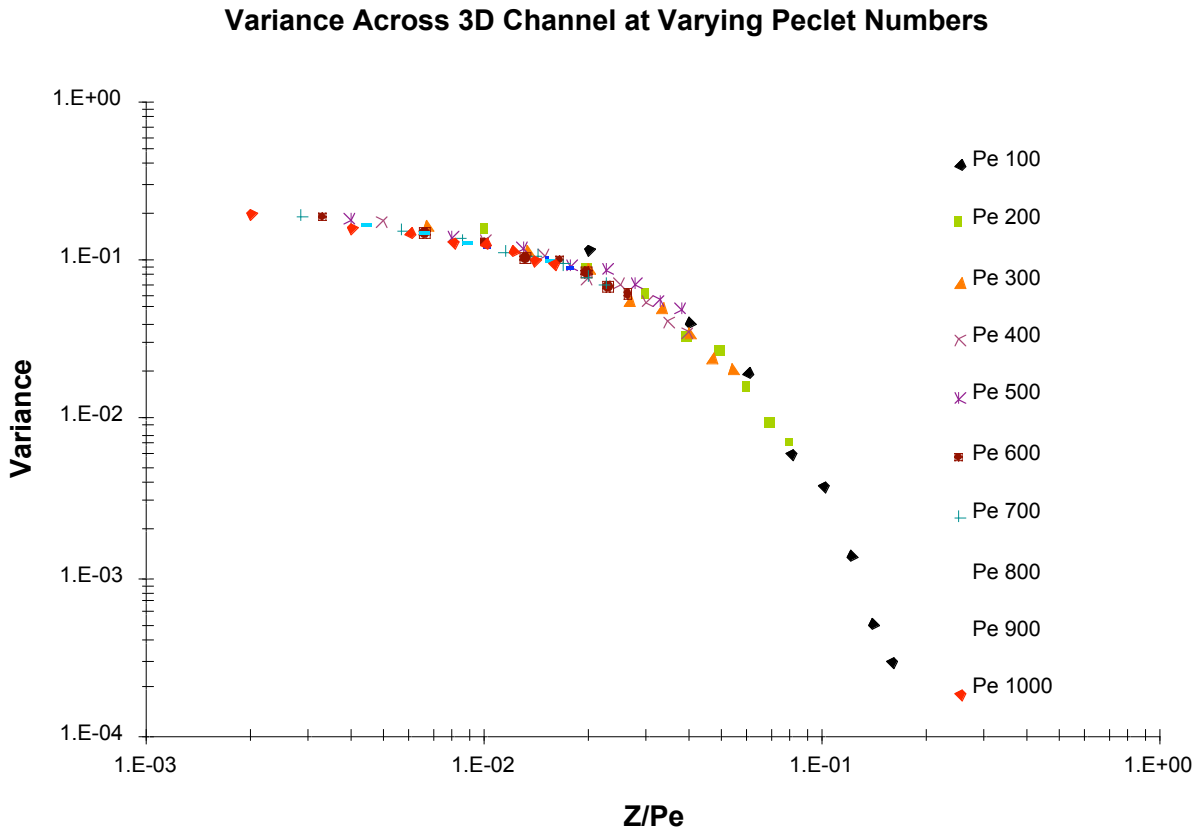

Figure 4: Shows the variances as a function of Z/Pe where Z the dimensionless distance from the inlet. Variances all lie on one curve regardless of the Peclet number. That is, variances are essentially the equivalent at the same Z/Pe.

With this behavior we are able to compare the mixing efficiencies of different geometries. When the rough channel mixer is compared to that of a T-sensor we find that the rough channels mix more efficiently as show in Figure 5.

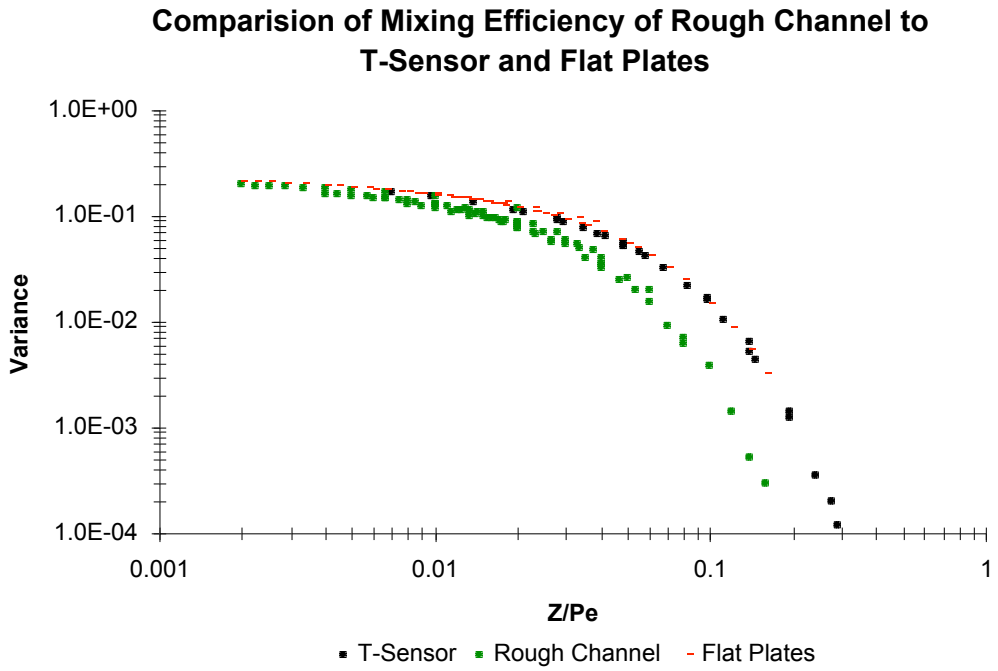

Figure 5: Concentration variances are shown in the above graph for the T-sensor, flat plates, and that of the rough channel.

When comparing the 2D and 3D results of the rough channel, the variances are essentially the same. The small differences may be due to mesh errors.

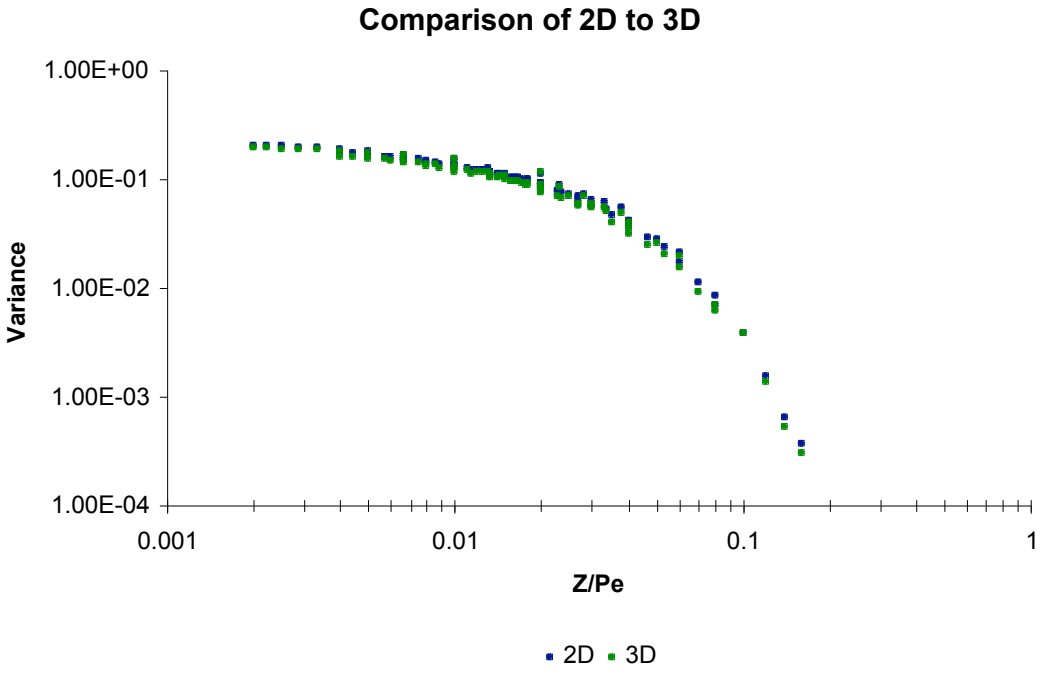

Figure 5: Concentration variances are shown in the above graph for the T-sensor, flat plates, and that of the rough channel.

When optical measurements were calculated the values did not reflect the mixing cup values in the rough channels, see Figure 7. This is due to the fact that a measurement taken along or near the wall of a ridge has a velocity of zero in the direction of flow. In the integral to determine the mixing cup concentration the section along the wall essentially disappears and thus the two values greatly differ along the rough channels.

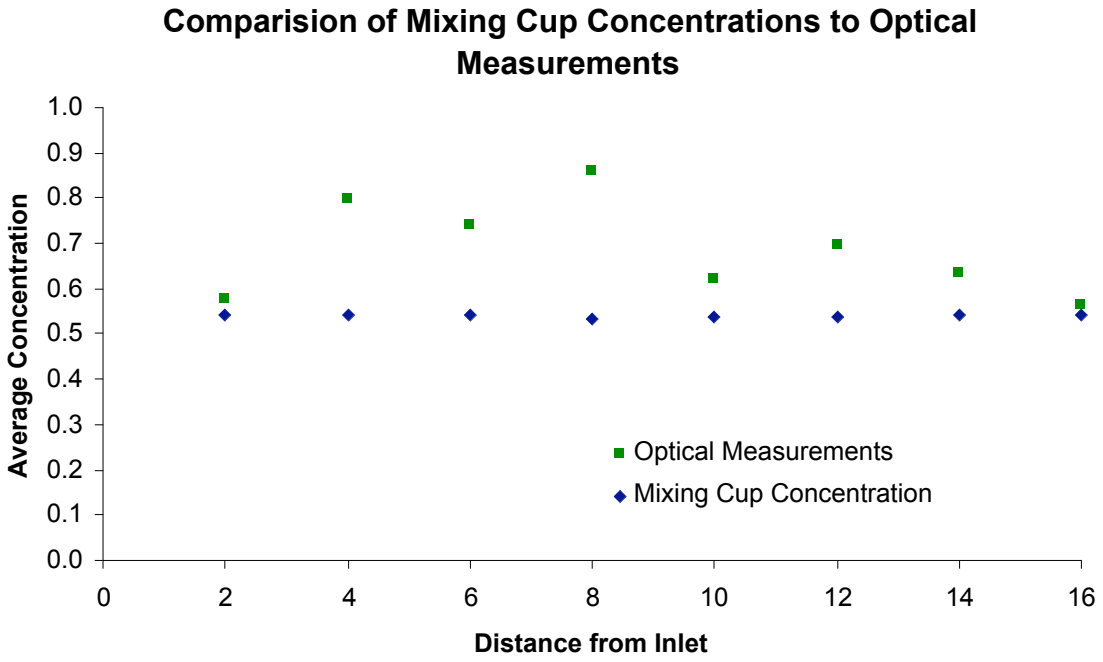

Figure 5: Mixing cup concentrations and average concentrations obtained from optical measurements are compared above.

Errors were considered in mesh sizes, the only values that were significantly different were the coptical and cmixing-cup the values for each respective variance were negligible as shown in the table below. Table 5 shows the values calculated at different mesh sizes for geometry C at Peclet number 100.

Elements	C_{mix}	$C_{variance(mix)}$	$C_{optical}$	$C_{variance}$ (optical)
8812	0.464	1.27E-04	0.465	1.34E-03
35248	0.483	1.28E-04	0.483	1.71E-04
52994	0.492	1.28E-04	0.492	1.71E-04

Table 6: shows the values calculated at different mesh sizes for geometry C at Peclet number 100.

It must also be noted that when the inlet concentration was non-uniform in the y direction mixing worsened and variances were in fact higher than that of flow between two flat plates.

Conclusions

It seems that the rough channel does not improve mixing unless the ridges are allowed to extend above the level of the lower plate. Although mixing is efficient in this particular geometry, optical measurements are not appropriate in the section containing the ridges and mixing cup concentrations must be used. The results also indicate that a two-dimensional representation of this geometry is sufficient enough to represent three dimensional results.

Recommendations

More analysis needs to be done on variations of these rough channels for further mixing. Specifically, in the 3D geometry, random dimensions should be considered in the third dimension. In addition, additional planes containing ridges, creating pillar like patterns should be considered.

APPENDIX

Tabulated Values:

	Peclet Number	C mix	C variance	C optical	C variance optical	Dimensionless Pressure Drop	Pressure Drop Pa
Flat Plates Elements: 22272 DOF: 45265	100	0.48306	0.000845	0.4824	0.00113	240	6.00
	200	0.48232	0.012857	0.4824	0.01715		
	300	0.48199	0.031928	0.4824	0.04253		
	400	0.48181	0.050329	0.4827	0.06687		
	500	0.48181	0.066136	0.4827	0.08747		
	600	0.48160	0.079354	0.4836	0.10429		
	700	0.48153	0.090401	0.4841	0.11789		
	800	0.48147	0.099711	0.4845	0.12894		
	900	0.48142	0.107645	0.4848	0.13799		
	1000	0.48138	0.114484	0.4851	0.14547		
Geometry A Elements: 6052 DOF: 12473	100	0.46368	0.001534	0.4637	0.00205	181	4.54
	200	0.46368	0.017344	0.4637	0.02314		
	300	0.46368	0.039001	0.4637	0.05195		
	400	0.46368	0.058478	0.4637	0.07759		
	500	0.46368	0.074544	0.4637	0.09829		
	600	0.46368	0.087624	0.4637	0.11462		
	700	0.46368	0.098352	0.4637	0.12749		
	800	0.46368	0.107271	0.4637	0.13774		
	900	0.46368	0.114796	0.4637	0.14600		
	1000	0.46368	0.121226	0.4637	0.15276		
Geometry B Elements: 7090 DOF: 14555	100	0.46426	0.001181	0.4643	0.00158	207	5.17
	200	0.46426	0.015167	0.4643	0.02024		
	300	0.46426	0.035586	0.4643	0.04745		
	400	0.46426	0.054515	0.4643	0.07248		
	500	0.46426	0.070421	0.4643	0.09315		
	600	0.46426	0.083547	0.4643	0.10973		
	700	0.46426	0.094428	0.4643	0.12300		
	800	0.46426	0.103550	0.4643	0.13368		
	900	0.46426	0.111300	0.4643	0.14238		
	1000	0.46426	0.117967	0.4643	0.14954		
Geometry C Elements: 8812 DOF: 18283	100	0.46493	0.000127	0.4649	0.00134	929	23.2
	200	0.46493	0.004974	0.4649	0.00664		
	300	0.46493	0.016935	0.4649	0.02261		
	400	0.46493	0.031248	0.4649	0.04171		
	500	0.46493	0.045120	0.4649	0.06016		
	600	0.46493	0.057634	0.4649	0.07667		
	700	0.46493	0.068642	0.4649	0.09101		
	800	0.46493	0.078260	0.4649	0.10330		
	900	0.46493	0.086671	0.4649	0.11381		
	1000	0.46493	0.094059	0.4649	0.12281		

3D Geometry C (short inlet and outlet) Elements: 40,825 Degrees of Freedom: 83,693 Pressure Drop of 31.8 Pa					
Pe #	Z/Pe	Cmix	Variance	Coptical	Variance
100	0.020	0.54	0.116967	0.5747	1.35E-01
	0.040	0.54	0.040665	0.6957	3.52E-02
	0.060	0.54	0.019782	0.6258	2.13E-02
	0.080	0.54	0.006114	0.6101	4.49E-03
	0.100	0.54	0.003841	0.5558	4.82E-03
	0.120	0.54	0.001397	0.5571	1.48E-03
	0.140	0.54	0.000521	0.5455	6.26E-04
	0.160	0.54	0.000301	0.5401	3.69E-04
200	0.010	0.55	0.151970	0.5771	1.68E-01
	0.020	0.55	0.088158	0.7648	7.45E-02
	0.030	0.55	0.060434	0.6873	6.34E-02
	0.040	0.55	0.032195	0.7122	2.47E-02
	0.050	0.55	0.026358	0.5855	3.24E-02
	0.060	0.55	0.015722	0.6037	1.65E-02
	0.070	0.55	0.009336	0.5714	1.10E-02
	0.080	0.55	0.007009	0.5500	8.44E-03
300	0.007	0.55	0.167005	0.5782	1.81E-01
	0.013	0.55	0.114272	0.7854	9.32E-02
	0.020	0.55	0.088336	0.7119	9.06E-02
	0.027	0.55	0.056805	0.7689	4.38E-02
	0.033	0.55	0.050666	0.6011	6.18E-02
	0.040	0.55	0.035778	0.6346	3.75E-02
	0.047	0.55	0.024923	0.5898	2.93E-02
	0.053	0.55	0.020459	0.5559	2.45E-02
400	0.005	0.55	0.174727	0.5786	1.90E-01
	0.010	0.55	0.129842	0.7916	1.03E-01
	0.015	0.55	0.106803	0.7230	1.07E-01
	0.020	0.55	0.076084	0.8016	5.81E-02
	0.025	0.55	0.070462	0.6095	8.51E-02
	0.030	0.55	0.054259	0.6543	5.67E-02
	0.035	0.55	0.040927	0.6019	4.81E-02
	0.040	0.55	0.035106	0.5592	4.20E-02
500	0.004	0.56	0.181841	0.5786	1.95E-01
	0.008	0.56	0.139915	0.7932	1.08E-01
	0.013	0.56	0.119465	0.7287	1.18E-01
	0.018	0.56	0.090635	0.8217	6.84E-02
	0.023	0.56	0.085765	0.6143	1.03E-01
	0.028	0.56	0.069668	0.6674	7.26E-02
	0.033	0.56	0.055237	0.6102	6.49E-02
	0.038	0.56	0.048670	0.5612	5.82E-02
600	0.003	0.56	0.186233	0.5785	2.00E-01
	0.007	0.56	0.146995	0.7934	1.11E-01
	0.010	0.56	0.128649	0.7318	1.25E-01
	0.013	0.56	0.102056	0.8349	7.61E-02

	0.017	0.56	0.097801	0.6172	1.16E-01
	0.020	0.56	0.082460	0.6769	8.58E-02
	0.023	0.56	0.067624	0.6164	6.64E-02
	0.027	0.56	0.060654	0.5626	7.26E-02
700	0.003	0.57	0.189654	0.5783	2.04E-01
	0.006	0.57	0.152260	0.7932	1.13E-01
	0.009	0.57	0.135579	0.7338	1.31E-01
	0.011	0.57	0.111207	0.8439	8.19E-02
	0.014	0.57	0.107383	0.6191	1.27E-01
	0.017	0.57	0.092973	0.6835	9.63E-02
	0.020	0.57	0.078207	0.6212	9.22E-02
	0.023	0.57	0.071042	0.5635	8.50E-02
800	0.003	0.57	0.192432	0.5781	2.07E-01
	0.005	0.57	0.156393	0.7933	1.15E-01
	0.008	0.57	0.141018	0.7352	1.35E-01
	0.010	0.57	0.118731	0.8505	8.64E-02
	0.013	0.57	0.115210	0.6203	1.35E-01
	0.015	0.57	0.101833	0.6886	1.05E-01
	0.018	0.57	0.087340	0.6253	1.03E-01
	0.020	0.57	0.080104	0.5643	9.59E-02
900	0.002	0.57	0.194760	0.5779	2.09E-01
	0.004	0.57	0.159838	0.7945	1.17E-01
	0.007	0.57	0.145459	0.7365	1.38E-01
	0.009	0.57	0.125074	0.8557	9.01E-02
	0.011	0.57	0.121755	0.6213	1.42E-01
	0.013	0.57	0.109406	0.6929	1.13E-01
	0.016	0.57	0.095281	0.6290	1.13E-01
	0.018	0.57	0.088044	0.5650	1.05E-01
1000	0.002	0.57	0.195738	0.5778	2.12E-01
	0.004	0.57	0.163001	0.7983	1.19E-01
	0.006	0.57	0.149295	0.7385	1.41E-01
	0.008	0.57	0.130577	0.8604	9.34E-02
	0.010	0.57	0.127412	0.6223	1.48E-01
	0.012	0.57	0.116042	0.6968	1.19E-01
	0.014	0.57	0.102264	0.6324	1.22E-01
	0.016	0.57	0.095068	0.5658	1.14E-01

Sample Calculations

Calculating pressure drop from non-dimensional pressure

$\eta = 10^{-3}\, Pa$

$x_s = 200\mu m$

$v_x = .005\frac{m}{s}$

$P = P^1 P_s$

$P_s = \frac{\eta v_s}{x_s}$

P^1 is the dimensionless pressure and P_s is the standard pressure. Thus for a dimensionless pressure of 928.8 we have:

$$P_s = \frac{10^{-3}\, Pa \times .005\frac{m}{s}}{200 \times 10^{-6}\frac{m}{s}} = .025 Pa$$

$$P = 928.8 \times .025 Pa$$

References

[1] Koplik, J., Ippolito, I., & Hulin, J. P. (1993). Tracer dispersion in rough channels: A two-dimensional numerical study. PHYSICS OF FLUIDS A FLUID DYNAMICS. 5 (6), 1333.

[2] Finlayson, B. A., Drapala P. W., Gebhardt, M., Harrison M. D., Johnson, B., Lukman, M., Kunaridtipol, S., Plaisted, T., Tyree Z., VanBuren, J., & Witarsa A. (2007). Micro Instrumentation. WILEY-VCH Verlag GmbH & Co.

[3] Finlayson, B. A. (2006). Introduction to chemical engineering computing. Hoboken, N.J.: Wiley-Interscience.